Fractal Geometries of Complementary Split-Ring Resonators

Vesna Crnojević-Bengin, *Member*, *IEEE*, Vasa Radonić, and Branka Jokanović, *Member*, *IEEE*

***Abstract*—Complementary split-ring resonators are typically used as negative-permittivity particles in microstrip left-handed structures. In this paper, novel complementary split-ring resonators that use square Sierpinski fractal curve are proposed and studied in detail. It is shown that the application of fractal geometries results in significant miniaturization of the metamaterial unit cell, in comparison with conventional and equivalent meander structures. Multiple fractal complementary split-ring resonators are also analyzed. The influence of different geometrical parameters and the order of the fractal curve on the performances are investigated, as well as the efficiency of excitation of the particles. When used in the design of left-handed transmission lines, fractal complementary split-rings improve frequency selectivity in the upper transition band, when compared to other non-fractal topologies.**

***Index Terms*—Metamaterials, split-ring resonators, fractals, microwave filters.**

I. Introduction

Recently, revolutionary results have been obtained in the field of metamaterials, artificial structures that exhibit electromagnetic properties generally not found in nature. Metamaterials are designed using sub-wavelength particles, whose size is typically smaller then one tenth of the propagating signal wavelength. Due to this fact, quasi-static analysis can be performed and the concept of artificial effective media can be applied. The structures obtained using this approach can be considered as a continuous medium with effective parameters, namely effective dielectric permittivity and effective magnetic permeability. By a proper choice of the type and geometrical arrangement of constituent sub-wavelength particles, the effective parameters of metamaterials can be made arbitrarily small or large, or even negative.

Double-negative or left-handed media, that simultaneously exhibit negative values of permittivity and permeability in a certain frequency range, were first theoretically studied by Veselago, [1]. However, the first structure that exhibits negative permittivity by decreasing the plasmon frequency into microwave range was proposed in mid nineties, [2]. Shortly afterwards, a particle called split-ring resonator, that provides negative permeability at microwave frequencies, was introduced, [3]. By superimposing these two structures, the existence of left-handed metamaterial was experimentally proved in 2001, [4].

An array of split-ring resonators exhibits the extreme values of effective magnetic permeability in the vicinity of resonance, namely highly positive/negative in a narrow band below/above the quasi-static resonant frequency of the rings. Although having a narrow frequency range with negative permeability, the configurations using split-ring resonators have driven a lot of attention, [5], [6]. An array of split-ring resonators exhibits filtering properties, and, when properly polarized, can inhibit signal propagation, thus offering an effective way to reject a frequency band in the vicinity of its quasi-static resonance, [7].

In the microstrip technology, split-ring resonators can only be etched on the upper substrate side, next to the host transmission line. In order to enhance the coupling, the distance between the line and the rings should be as small as possible. Therefore, square or rectangle geometries are typically used instead of the originally proposed circular ones. The microstrip line loaded with split-ring resonators is a single-negative medium, and therefore exhibits a stop-band characteristic.

With the aim of further miniaturization, other sub-wavelength particles have been recently proposed, such as the broadside coupled split-ring resonator, [8], and the spiral resonator, [9], [10], as well as multiple geometries, namely the multiple split-ring resonator, and the multiple spiral resonator, [11], [12]. Although solutions utilizing multiple spiral resonators exhibit the highest potential for miniaturization, they also suffer from high insertion loss.

Applying the Babinet principle, a complementary structure was proposed in [13], namely the complementary split-ring resonator. In the microstrip technology, complementary split-ring resonators are etched in the ground plane, beneath the microstrip, with their axes parallel to the vector of the electric field, thus contributing to the negative effective dielectric permittivity of the structure. In order to obtain the left-handed behaviour, effective negative permeability has to be introduced to the structure. This is achieved by periodically etching capacitive gaps in the conductor strip.

In this paper, novel sub-wavelength particles are presented based on the application of fractal geometries to

Manuscript received September 21, 2007. This work was supported in part by the Ministry for Science and Environmental Protection of Republic of Serbia under Contract 401-00-213/2006-01/05, and by EUREKA project number E!3853.

V. Crnojević-Bengin and V. Radonić are with the Faculty of Technical Sciences, University of Novi Sad, Serbia (phone: 381-21-485-2553; fax: 381-21-475-0572; e-mail: bengin@uns.ns.ac.yu, vasaradonic@eunet.yu).

B. Jokanović is with the IMTEL-Komunikacije, Belgrade, Serbia (e-mail: branka@insimtel.com).

complementary split-ring resonators, [14]. The electromagnetic behaviour of the proposed particles is investigated from the point of view of the size reduction, performances and coupling to the host transmission line.

In Section II, the possibilities of application of two-dimensional fractal curves in sub-wavelength particle design are analyzed. The definition of fractal dimension is given and it is described why square Sierpinski fractal curve has been chosen to substitute conventional square complementary split-ring resonator geometry. The configuration of the proposed square Sierpinski complementary split-ring resonators is also shown.

In Section III new metamaterial unit cells based on the application of square Sierpinski complementary split-ring resonators and gaps etched in the microstrip are presented. The influence of different geometrical parameters to the performances of the proposed unit cells is analyzed in detail, and compared with other similar but non-fractal geometries. The efficiency of excitation of square Sierpinski complementary split-ring resonator by axial electric field is analyzed as a function of geometry of the ring. Unit cells that use multiple square Sierpinski complementary split-ring resonators are investigated for the first time, as well as the influence of the fractal curve order on performances of the proposed unit cells. The electrical model of the unit cell and the procedure for circuit parameter extraction are given, and circuit parameters are extracted for all structures. Different behaviour of conventional square and fractal rings is illustrated by dispersion diagrams.

In Section IV, the proposed unit cells are applied to the design of left-handed transmission lines. The simulation and measurement results are given, and the performances of all fractal-based structures are compared with those obtained by configurations that use conventional square complementary split-ring resonators with the same dimensions. The conclusion is given in Section V.

II. Fractal Curves

The fractal curves have been known since the end of 19th century, when Peano constructed a continuous curve that passes through every point of a given region, [15]. The fractal curves are generated in an iterative manner by successive repetition of one geometrical shape with the other (that often is a collection of scaled copies of the first shape). After each iteration, a fractal curve of the higher order is obtained, longer then the previous one, which better fills the area in which it is generated. This space-filling property offers high potentials for miniaturization of passive microwave circuits, because, theoretically, the application of fractal curves allows the design of infinite-length lines on a finite substrate area.

Our recent results have shown that the application of fractal curves results in very compact high-Q microstrip resonators and filters, [16], [17], which outperform all other non-fractal solutions. This is due to the increase of the overall length of the microstrip line on a given substrate area as well as to the specific line geometry.

The fractal geometries have also been utilized for the design of wire structures used in applications such as miniaturized antennas [18]-[21], frequency selective surfaces, [22], high-impedance surfaces, [23], [24], left-handed metamaterials, [25], and radio-frequency identification, [26]. In the metamaterial designs, a bulk effective medium is formed by embedding a great number of identical sub-wavelength fractal-shaped inclusions within a host medium. Also, an extended class of space-filling wire structures based on grid-graph Hamiltonian paths and cycles has been investigated, [27]. Possible practical applications of the results mentioned above are envisaged in the design of thin absorbing screens, and ground-planes for antennas. However, they are not directly applicable to the split-ring design, because, in the latter case, some additional characteristics of the fractal curves are required.

The fractal curves are characterized by fractal, i.e. non-integer, dimension. The dimension of every fractal curve is the number between 1 and 2, and can be understood as a measure of the space-filling ability of the fractal curve. The dimension D can be determined as a logarithmic ratio between the number of self-similar segments obtained from one segment after each iteration, k, and the number of segments obtained from one segment in each iteration, r:

$$D = \frac{\log k}{\log r} \tag{1}$$

A great number of fractal curves are known today. Trying to determine which fractal curve would suit best given application, some criterion has to be introduced. With the aim of further miniaturization, the fractal dimension is chosen as the most important characteristic. The higher the fractal dimension, the better fractal curve fills the given area, therefore achieving higher compactness. Three fractal curves are known that have fractal dimension equal to 2 (i.e. the maximum value): Peano, Hilbert and square Sierpinski fractals, shown in Fig. 1.

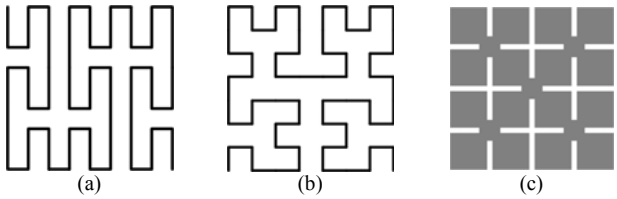

Fig. 1. Fractal curves with the dimension equal to 2: (a) Peano, (b) Hilbert, and (c) square Sierpinski.

Since Hilbert and Peano fractals are open curves that have ends on the opposite sides, they are convenient for usage in structures such as end coupled microstrip resonators, [16], or metasurfaces, [23]-[25], [27]. However, in the case of split-ring resonators, some specific characteristics of the fractal curve are required. In order to ensure the best performances of a split-ring, a trade-off is needed between increased inductance and capacitance of the particle (i.e. maximized line length) and its geometry. The geometry of the particle has to

allow for efficient excitation, i.e. the particle has to have an unoccupied area in its middle section.

Square Sierpinski fractal consists of squares that fill the given area. It resembles Minkowski fractal, but has ratio between inner and outer squares equal to 2:3. Furthermore, in the case of square Sierpinski fractal, inner and outer squares overlap, thus creating a denser structure. Square Sierpinski fractal curves of the first three orders are shown in Fig. 2.

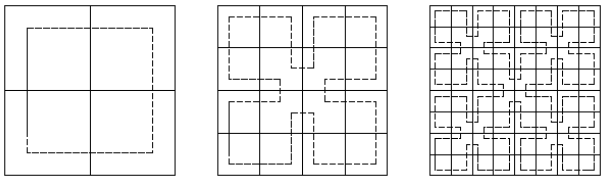

Fig. 2. Generation of square Sierpinski fractal curve – first three iterations.

Sierpinski fractal curve of the second order with the relevant dimensions is shown in Fig. 3(a), where *a*, *b* and *g* denote size of its segments. According to the rule of square Sierpinski fractal generation, the following relations are obtained:

$$b = 3 \cdot g \qquad a = 2 \cdot g \tag{2}$$

A closed curve can be designed that follows the outer perimeter of the square Sierpinski fractal curve that can straightforwardly be used as a substitute to the conventional square complementary split-ring resonator.

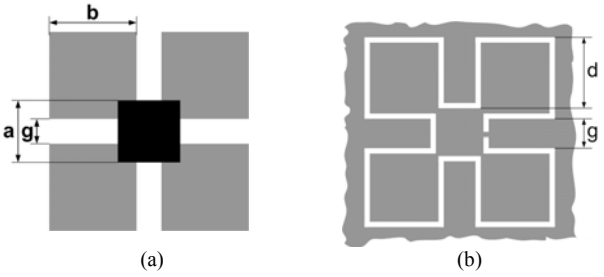

Fig. 3. (a) Square Sierpinski fractal curve of the second order, (b) Single square Sierpinski complementary split-ring resonator.

The square Sierpinski complementary split-ring resonator, designed to follow the outer perimeter of the fractal curve, is shown in Fig. 3(b), where *d* denotes length of insets. The etched line having minimal width achievable by the conventional PCB technology is used, equal to 100 μm. It is well known, [3], that by the usage of two concentric rings with slits on the opposite sides, resonant frequency of the structure can be significantly reduced. In order to investigate influence of the number of concentric rings, multiple ($N \geq 2$) square Sierpinski complementary split-ring resonators will also be analyzed. The separation between concentric rings is chosen to be the minimal achievable, i.e. equal to 100 μm, to enhance the coupling.

To facilitate insertion of more then one concentric square Sierpinski complementary split-ring inside the structure, while keeping the overall dimensions of the particle fixed, gap *g* has to be reduced. This also results in a decrease of length of insets *d*. Square Sierpinski complementary split-ring resonators obtained in this manner are shown in Fig. 4, for the case $N=2$, 3 and 4, respectively, where *N* denotes number of concentric complementary rings.

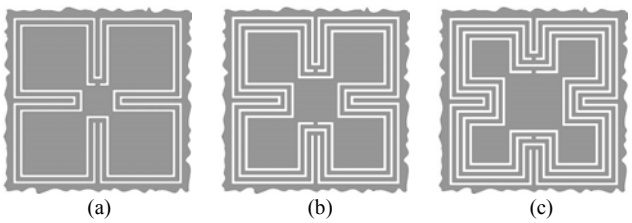

Fig. 4. Multiple square Sierpinski complementary split-ring resonators with *N* concentric rings: (a) $N=2$, (b) $N=3$, (b) $N=4$.

III. Left-Handed Unit Cells that Use Square Sierpinski Complementary Split-Ring Resonators

A. Configuration

In order to obtain left-handed behaviour, two particles need to be combined in a unit cell: complementary split-ring resonator that will provide negative effective permittivity and a gap in the microstrip that will provide negative effective permeability. In order to achieve high magnetic coupling between the line and the ring at resonance, complementary split-ring resonators are etched in the ground layer under the gaps. The proposed unit cell is shown in Fig. 5, where both top (dark grey) and bottom (light grey) conductive layers are shown. The unit cell was simulated on a 1.27 mm thick Taconic CER-10 substrate, with $\varepsilon_r = 9.8$ and dielectric loss tangent equal to 0.0025. The outer dimensions of a single square Sierpinski complementary split-ring resonator are equal to 5.1 x 5.1mm, i.e. $\lambda_g/15$ x $\lambda_g/15$ on a given substrate.

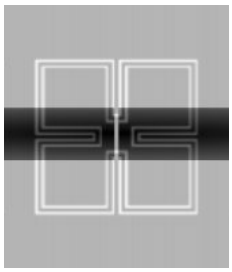

Fig. 5. Left-handed unit cell that consists of $N=2$ square Sierpinski complementary split-ring resonator and a gap in the host microstrip line.

B. Influence of Different Geometrical Parameters

In order to analyze the influence of different geometrical parameters on the performances of square Sierpinski

complementary split-ring resonator, lengths of insets d are varied. Fig. 6 shows two extreme cases: d=1800 μm is the original square Sierpinski complementary split-ring resonator, i.e. the one whose dimensions correspond to the rule of generation of the fractal curve, and d=600 μm corresponds to the minimum achievable inset. Furthermore, to highlight the specific features of fractal curves, the proposed unit cell is compared with a cell that uses conventional square complementary split-ring resonator (CSRR) as well as with a cell that uses meander shaped complementary split-ring resonator (M CSRR), shown in Fig. 6(c). Meander complementary split-ring resonator has been designed to occupy precisely the same area as the original square Sierpinski complementary split-ring resonator, as well as to have exactly the same circumference of the rings. The performances of the proposed structures are determined using EMSight, EM simulator in Microwave Office and the comparison of simulation results for the lossy case is given in Table I, where f_r denotes resonant frequency of the unit cell, BW is a 3 dB bandwidth, s_{21}^0 and s_{11}^0 are insertion loss and reflection at resonant frequency, Q_L is loaded and Q_U is unloaded quality factor.

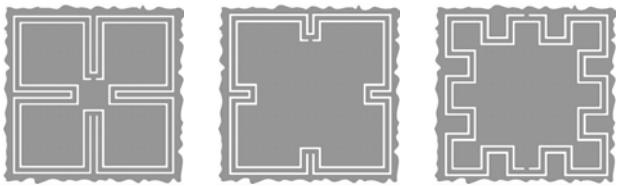

Fig. 6. Analyzed topologies: (a) square Sierpinski complementary split-ring resonator, d=1800 μm, (b) square Sierpinski complementary split-ring resonator, d=600 μm, and (c) meander complementary split-ring resonator with the same circumference and the same area of the rings as the resonator depicted in (a).

TABLE I
SIMULATION RESULTS FOR UNIT CELLS THAT USE N=2 SQUARE SIERPINSKI COMPLEMENTARY SPLIT-RING RESONATORS (SS CSRR) WITH DIFFERENT LENGTHS OF INSETS, COMPLEMENTARY SPLIT-RING RESONATOR (CSRR) AND MEANDER COMPLEMENTARY SPLIT-RING RESONATOR (M CSRR)

	SS CSRR			CSRR	M CSRR
d [μm]	1800	1200	600	-	-
f_{c1} [GHz]	1.34	1.51	1.72	2.03	1.57
BW [MHz]	97.7	126	177.3	256.6	127
BW [%]	7.29	8.34	10.31	12.64	7.38
s_{21}^0 [dB]	-5.02	-3.86	-2.9	-2.23	-3.83
s_{11}^0 [dB]	-8.95	-11.2	-14.3	-20.2	-12
Q_L	13.72	11.98	9.7	7.91	12.36
Q_U	20.01	20.35	19.91	19.7	21.1

Since decreasing d results in shorter circumference of the square Sierpinski complementary split-ring resonator, its resonant frequency increases, due to the reduced inductance and capacitance of the particle. However, in all cases a significant reduction of the resonant frequency in comparison to the conventional complementary split-ring resonator can be observed, ranging from 15% to 34%, for different length of inset d. Furthermore, all fractal structures exhibit higher values of the quality-factor then the conventional ring.

The comparison of unit cells that use meander complementary split-ring resonator and the original (d=1800 μm) square Sierpinski complementary split-ring resonator, gives the evidence to improved performances of the fractal geometries in comparison with similar but non-fractal ones. Although both structures have exactly the same line length and occupy precisely the same area, resonant frequency of the unit cell that uses square Sierpinski complementary split-ring resonator is approximately 15% lower, due to the specific shape of the fractal curve.

Therefore, it can be concluded that fractal geometries with the original dimensions perform better in terms of miniaturization than the modified ones, as well as better then similar non-fractal structures. Although square Sierpinski complementary split-ring resonator with insets equal to 600 μm shows significantly better insertion loss then its counterpart with maximized insets, it is less interesting from the point of view of miniaturization. That is why in the remaining part of this paper, only fractal structures with the original dimensions will be considered, modified only to the minimal extent to allow the insertion of inner concentric rings. However, it should be kept in mind that fractal rings can achieve significantly lower insertion loss if insets smaller then the original ones are used, at the price of somewhat increased dimensions of the unit cell.

C. *Efficiency of Excitation*

Complementary split-ring resonator is excited by axial electric field that penetrates the area in the centre of the ring. In the case of square Sierpinski complementary split ring resonator, this area is partially occupied by the ring. In this section, the influence of fractal geometry on the efficiency of excitation is analyzed.

Two unit cells with similar geometries are simulated: one that uses the proposed square Sierpinski complementary split-ring resonator, and the other that uses quasi square Sierpinski complementary split-ring resonator. In the latter case, two opposite insets are rotated outwards, Fig. 7(b), so that the size of the homogenous metallic segments within the ring is increased for approximately 15%. It is commonly believed that such structure will allow more efficient excitation and result in stronger coupling between the host microstrip line and the ring.

The simulation results shown in Table II reveal that the resonant frequency is almost unchanged, which is expected due to the fact that both structures have approximately the same inductance and capacitance. However, the other performances are almost unchanged as well: the unit cell with quasi square Sierpinski complementary split-ring resonators exhibits very slightly wider 3 dB bandwidth, somewhat smaller insertion loss in the pass-band, and lower quality factors. All these can be attributed to enhanced excitation, i.e. better coupling between the ring and the microstrip, which is

the direct result of increased area of the homogenous metallic segments within the ring. However, all differences are so small that we concluded that the shape of the fractal ring does not significantly influence the excitation. The increased insertion loss that fractal rings exhibit in comparison to the conventional ones (Table I) is not due to deteriorated excitation, but is the consequence of the significantly increased length of the fractal ring. This conclusion is also supported by additional experiments performed with similar structures, such as square Sierpinski complementary split-ring resonator rotated for 45 degrees in respect to the original one. In all cases, almost negligible differences in performances were observed although area available for excitation was significantly changed.

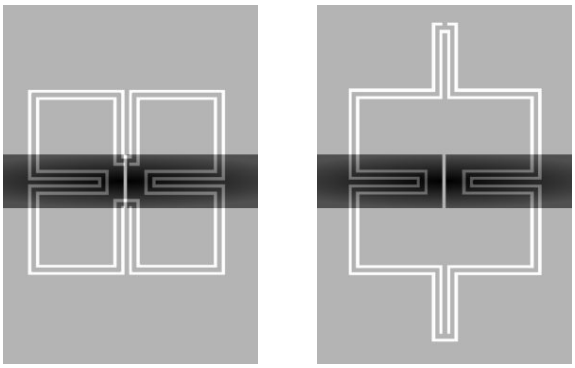

(a) (b)

Fig. 7. Unit cell that uses: (a) square Sierpinski complementary split-ring resonator, (b) quasi square Sierpinski complementary split-ring resonator.

TABLE II
SIMULATION RESULTS FOR UNIT CELLS THAT USE SQUARE SIERPINSKI COMPLEMENTARY SPLIT-RING RESONATORS (SS CSRR) AND QUASY SQUARE SIERPINSKI COMPLEMENTARY SPLIT-RING RESONATORS (Quasi SS CSRR)

	SS CSRR	Quasi SS CSRR
f_c [GHz]	1.35	1.32
BW [MHz]	97.5	97.6
BW [%]	7.22	7.39
s_{21}^0 [dB]	-5.01	-4.86
s_{11}^0 [dB]	-8.95	-9.72
Q_L	13.85	13.52
Q_U	20.23	20.08

D. *Unit Cells That Use Multiple Square Sierpinski Complementary Split-Ring Resonators*

The influence of additional inner concentric rings of square Sierpinski complementary split-ring resonator on performances of the unit cell is analyzed in Table III for the lossy case.

In the case of the conventional complementary square split-ring resonators, adding multiple split-rings significantly reduces resonant frequency, due to the increased inductance of the structure, [11], [12]. In the case of fractal curves, this holds only when the structures with N=1 and N=2 rings are compared, due to considerably increased capacitance of the unit cell. Adding more then two concentric complementary split-rings changes the resonant frequency only for a few percents, owing to the specific space-filling property of the fractal curves. However, when the number of concentric rings is increased, the second harmonic is significantly shifted towards the higher frequencies, up to more then three times the first resonance, thus resulting in a much wider stop band.

TABLE III
SIMULATION RESULTS FOR UNIT CELLS THAT USE MULTIPLE SQUARE SIERPINSKI COMPLEMENTARY SPLIT-RING RESONATORS

N	1	2	3	4
f_{c1} [GHz]	1.94	1.34	1.33	1.36
BW [MHz]	159.5	97.7	94.4	121.7
BW [%]	8.2	7.3	7.1	8.9
s_{21}^0 [dB]	-4.27	-5.02	-5.04	-4.43
s_{11}^0 [dB]	-3.24	-8.95	-8.25	-9.21
f_{c2} [GHz]	3.08	2.86	3.47	4.25
f_{c2}/f_{c1}	1.58	2.13	2.61	3.11
Q_L	12.19	13.71	14.09	11.22
Q_U	19.48	20.02	20.52	17.54

E. *Influence of the Fractal Curve Order*

Unit cells with N=1 and N=2 square Sierpinski complementary split-rings of the third order have been simulated for the lossy case, to analyze the influence of the order of the fractal curve. The overall dimensions of square Sierpinski complementary split-ring resonators are unchanged, i.e. equal to 5.1 x 5.1 mm. Both structures are shown in Fig. 8, while their performances are compared in Table IV.

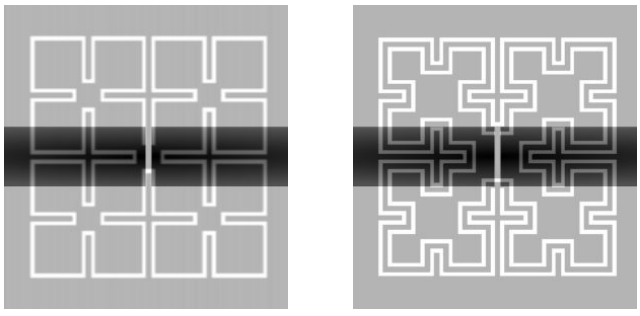

(a) (b)

Fig. 8. Unit cells that use (a) N=1 and (b) N=2 concentric square Sierpinski complementary split-rings with the fractal curve of the third order.

By comparing the results for N=1 from Table III and Table IV, it can be seen that the application of the fractal curves of the higher order results in the reduction of the resonant frequency of almost 20%, and therefore allows the design of more compact unit cells. When the number of concentric rings N is increased, the proposed unit cell scales down to $\lambda_g/20$ x $\lambda_g/20$. The increased losses are direct result of the increased

line length, but at the same time the second harmonic is shifted at more then four times the first resonance.

TABLE IV
SIMULATION RESULTS FOR UNIT CELLS THAT USE *N* SQUARE SIERPINSKI COMPLEMENTARY SPLIT-RINGS OF THE THIRD ORDER

N	1	2
f_{c1} [GHz]	1.56	1.14
BW [MHz]	58.2	57.7
BW [%]	3.7	5.1
s_{21}^0 [dB]	-5.56	-8.85
s_{11}^0 [dB]	-6.38	-3.76
f_{c2} [GHz]	3.86	4.8
f_{c2}/f_{c1}	2.47	4.21
Q_L	26.89	19.69
Q_U	37.24	22.64

F. Electrical Model and Parameter Extraction

The proposed unit cell can be modelled by the equivalent circuit shown in Fig. 9 regardless of the type of the complementary split-ring resonator used (conventional or Sierpinski) or of the number of concentric rings. This model is valid under the assumption that the size and the distance between the adjacent rings are both electrically small, which is the case. The complementary split-ring resonator is modelled by the parallel resonant circuit (with inductance L_r and capacitance C_r), electrically coupled to the host microstrip line through the line capacitance C_c. The microstrip line is modelled by the inductance L, while the capacitance C_g models the series gap in the microstrip.

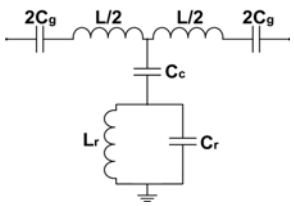

Fig. 9. Equivalent circuit of the proposed unit cell.

Values of the elements of equivalent circuit are obtained from the frequency response of the unit cell, for the lossless case. Two specific frequencies are used in the process: the resonant frequency of the complementary split-ring, f_0, and the transmission zero frequency f_z, at which the impedance of the shunt branch is equal to zero.

At the resonant frequency of the complementary split-ring,

$$f_0 = \frac{1}{2\pi\sqrt{L_r C_r}}, \tag{3}$$

the impedance seen from the input port is given by the impedance of the output port, equal to 50Ω, enlarged for the reactive impedance of the series branch. This frequency can easily be determined from the Smith Chart. The line inductance L is estimated using a transmission line calculator, and the capacitance C_g is determined based on the value of series reactance.

The transmission zero frequency,

$$f_z = \frac{1}{2\pi\sqrt{L_r\left(C_r + C_c\right)}} \tag{4}$$

is also easily obtained from full-wave simulations. Equations (3) and (4) can be rewritten in the following form:

$$L_r = \frac{\left(\frac{f_0}{f_z}\right)^2 - 1}{\left(2\pi f_0\right)^2} \cdot \frac{1}{C_c}, \tag{5}$$

$$C_r = \frac{C_c}{\left(\frac{f_0}{f_z}\right)^2 - 1}, \tag{6}$$

thus giving dependence of L_r and C_r from C_c. The response of the electrical model is fitted to the one obtained from full-wave simulations by changing value C_c, using Variable Tuner tool available in Microwave Office. To validate the parameter extraction method and the obtained values of circuit elements, the responses are compared in Fig. 10, for both fractal and conventional unit cells with two concentric rings (*N*=2). It can be seen that the electrical model describes electromagnetic behaviour of the unit cell very accurately, and in a wide range of frequencies, up to the second harmonic. The second harmonic exists in electromagnetic responses due to the distributed nature of the structures. A more complicated electrical model could be developed that would accurately predict the second resonance too. However, since the second harmonic is not of interest for the current application, the simplified model shown in Fig. 9 is used.

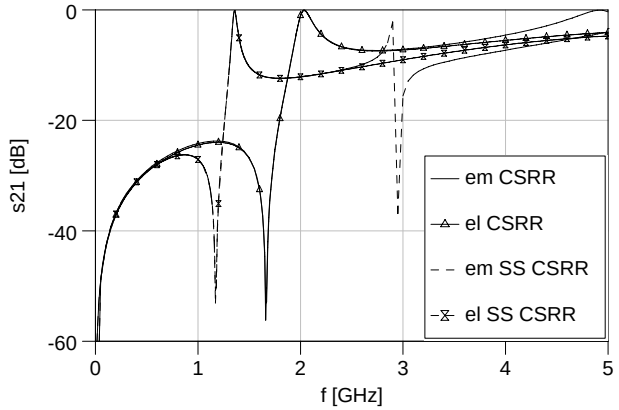

Fig. 10. Comparison of responses obtained from full-wave electromagnetic simulations (em) and electrical simulations (el) of model shown in Fig. 9, for unit cells that use square Sierpinski complementary split-ring resonator (SS CSRR) and complementary split-ring resonator (CSRR) with two concentric rings.

Table V contains the extracted values of circuit elements for unit cells that use multiple square Sierpinski complementary split-ring resonators. To illustrate the differences which occur when fractal geometry is used, extracted parameters for conventional multiple square complementary split-ring resonators that occupy the same area as their fractal counterparts are shown in Table VI, together with the extracted values for the meander complementary split-ring shown in Fig. 6(c). In both tables, N denotes the number of concentric rings.

TABLE V

EXTRACTED PARAMETERS FOR UNIT CELLS THAT USE MULTIPLE SQUARE SIERPINSKI COMPLEMENTARY SPLIT-RING RESONATORS DESIGNED WITH FRACTAL CURVES OF THE SECOND AND THE THIRD ORDER

Order	II			III	
N	2	3	4	1	2
L [nH]	2.49	2.37	2.3	2.11	2.08
C_g [pF]	0.329	0.354	0.389	0.296	0.304
C_c [pF]	2.49	3.13	3.64	2.36	2.63
L_r [nH]	2.786	2.361	2.132	1.114	2.326
C_r [pF]	**4.095**	**5.044**	**5.222**	**8.542**	**7.434**

TABLE VI

EXTRACTED PARAMETERS FOR UNIT CELLS THAT USE MULTIPLE SQUARE COMPLEMENTARY SPLIT-RING RESONATORS AND N=2 MEANDER COMPLEMENTARY SPLIT-RING RESONATOR WITH THE SAME DIMENSIONS AS ITS FRACTAL COUNTERPART.

	SQUARE COMPLEMENTARY SPLIT-RINGS			MEANDER
N	2	3	4	2
L [nH]	2.22	2.08	1.87	2.48
C_g [pF]	0.325	0.338	0.341	0.327
C_c [pF]	2.52	2.81	2.71	2.47
L_r [nH]	1.774	2.282	2.815	2.2
C_r [pF]	**2.63**	**2.47**	**2.23**	**3.75**

By comparing results in Tables V and VI (square complementary split-rings) for N=2, it can be seen that the application of fractal geometry increases the inductance of the split-ring for approximately 57% and it's capacitance for more then 55%, for the fixed overall dimensions of the ring. This is due to the significant increase of the ring's circumference. Host microstrip line inductance, gap capacitance and coupling capacitance remain almost unchanged. A comparison between N=2 fractal and meander geometries reveals significant advantage of the former: although both complementary split-rings occupy exactly the same area and have exactly the same circumference of the rings, square Sierpinski exhibits both larger inductance and larger capacitance, due to the specific shape of the fractal curve. Again, this gives evidence to superior performances of the fractal geometries in comparison with non-fractal ones.

Different behaviour of fractal and non-fractal structures can be observed for higher values of N. In the case of conventional square complementary split-rings, the inductance L_r significantly increases with N, which is expected due to the increased total length of the rings. In the same time, the capacitance C_r decreases slightly due to reduced dimensions of the most inner ring, [7]. On the other hand, quite the opposite effect is observed in the case of fractal ring geometry: the inductance L_r decreases and the capacitance C_r significantly increases with N. This can be explained in the following manner. Although the circumference of each ring is increased due to its fractal shape, the total inductance is reduced because of the existence of line segments with opposite currents in each ring (such as insets with length d, Fig. 3(b)). However, the existence of insets does not influence the resulting capacitance between the rings: fractal concentric rings with almost doubled circumference result in more then two times bigger capacitance, when compared to the conventional square case.

This conclusion also holds for complementary split-rings that use fractal curve of the third order: although the total line length is significantly increased in comparison to the rings that use fractal curves of the second order, the inductance L_r is almost unaffected. Again, this is explained by the existence of a great number of parallel line segments with opposite currents that reduce the total inductance. The observed reduction of the resonant frequency is mainly due to the increased capacitance of the structure.

Different behaviour of conventional square and fractal rings is also noticeable from the dispersion diagrams shown in Fig. 11. The dispersion relation has been calculated from the equivalent circuit:

$$\cos \beta l = 1 + \frac{C_c}{2C_g} \quad \frac{(1-\omega^2 LC_g)(1-\omega^2 L_r C_r)}{1-\omega^2 L_r (C_c + C_r)}. \qquad (7)$$

Although both structures are unbalanced and operate in somewhat different frequency bands, it can be seen that increasing the number of concentric rings N has different influence on the dispersion: it increases the stop band in the conventional case and decreases it in the fractal case. Furthermore, the left-handed pass band is almost unaffected by changing N in the fractal case.

IV. LEFT-HANDED MICROSTRIP LINES THAT USE SQUARE SIERPINSKI COMPLEMENTARY SPLIT-RING RESONATORS

A. Left-Handed Microstrip Lines That Use Unit Cells With N=2 Square Sierpinski Complementary Split-Ring Resonators

One possible application of the proposed unit cells is in the design of left-handed transmission lines. Such transmission lines can be characterized as narrow band pass filters with a sharp transition in the lower band edge. However, in the case of conventional square complementary split-ring resonators, they exhibit poor frequency selectivity in the upper transition band.

In Table VII the simulation results for the lossy case are compared for left-handed microstrip lines that use unit cells with N=2 square Sierpinski complementary split-ring resonators with insets equal to d=1800 μm and d=600 μm,

and conventional N=2 complementary split-ring resonators. The structures are characterized in terms of a band pass filter, where f_c denotes central frequency, BW is a 3 dB bandwidth, s_{21}^0 is insertion loss in the pass band, Q_L is loaded and Q_U is unloaded quality factor.

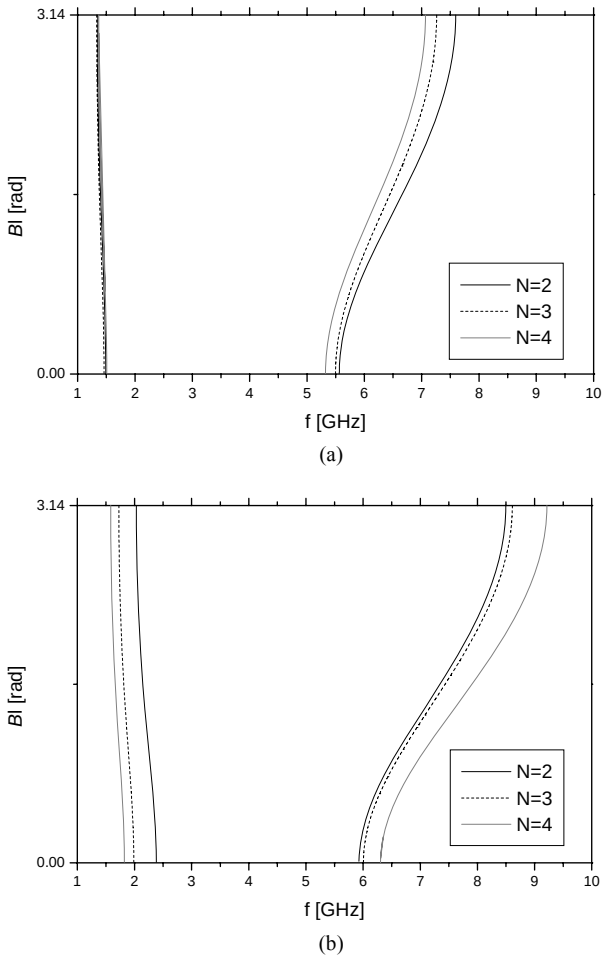

Fig. 11. Dispersion diagrams of left-handed unit cells that use: (a) square Sierpinski complementary split-ring resonators with fractal curve of the second order, and (b) conventional square complementary split-ring resonators.

TABLE VII

COMPARISON OF SIMULATION RESULTS FOR LEFT-HANDED TRASMISSION LINES THAT USE SQUARE SIERPINSKI COMPLEMENTARY SPLIT-RING RESONATORS (SS CSRR) AND CONVENTIONAL SQUARE COMPLEMENTARY SPLIT-RING RESONATORS (CSRR) WITH TWO CONCENTRIC RINGS (N=2)

	SS CSRR	SS CSRR	CSRR
d [μm]	1800	600	-
f_c [GHz]	1.365	1.765	2.123
BW [MHz]	69.5	164	170.95
BW [%]	5.1	9.29	8.05
s_{21}^0 [dB]	-12.8	-6.48	-5.62
s_{11}^0 [dB]	-8.95	-14.3	-20.2
Q_L	19.6	10.76	12.4
Q_U	20.7	13.88	17.1

By comparing results obtained for the conventional square complementary split-ring resonators with those corresponding to the original fractal geometries (d=1800 μm), it can be seen that the application of square Sierpinski complementary split-ring resonators reduces central frequency for more than 35%, for the same overall dimensions of the unit cell, at the price of reduced bandwidth and increased insertion loss. However, if the fractal geometry with d=600 μm insets is used instead, reduction of resonant frequency of approximately 17% is still achieved, while other performances are preserved. This demonstrates the potential that fractal geometries have for miniaturization.

In order to validate simulation results, left-handed microstrip lines that use square Sierpinski complementary split-ring resonators with the original dimensions and the conventional square complementary split-ring resonators were fabricated in standard PCB technology on a 1.27 mm thick Taconic CER-10 substrate. Photographs of top and bottom layers of both fabricated structures are shown in Fig. 12.

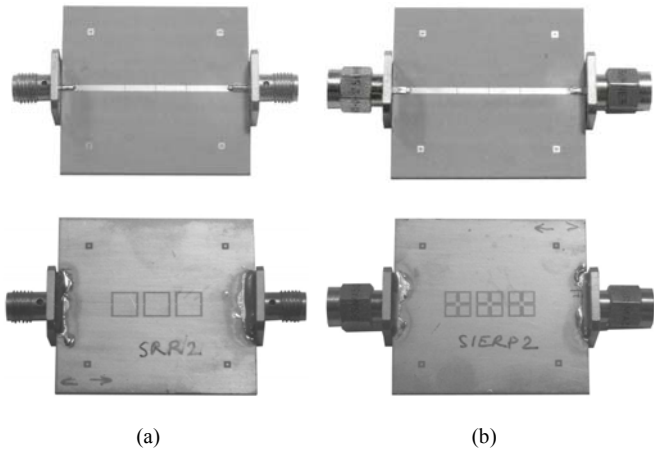

Fig. 12. Top (upper) and bottom (lower) sides of fabricated structures using: (a) conventional square complementary split-ring resonators, (b) square Sierpinski complementary split-ring resonators.

The simulation and measurement results for both structures are shown in Fig. 13. A good agreement with simulations can be observed, except for a shift in frequency approximately equal to 10% that have occurred in both cases. Since manufacturer specifications for substrate material allow εr variations in the range +/- 0.5 as well as variations of substrate thickness, this can be explained by the discrepancy between the actual and the simulated values of the dielectric constant and substrate thickness. The measured insertion losses correspond well to the simulated ones.

Fig. 14 shows the results of measurements performed up to 6GHz, for both structures. It can be seen that, unlike the conventional one, the configuration that uses square Sierpinski complementary split-ring resonators shows sharp transition on both sides of the pass band. Furthermore, it suppresses the second harmonic below 22dB, thus creating a wide and deep stop band.

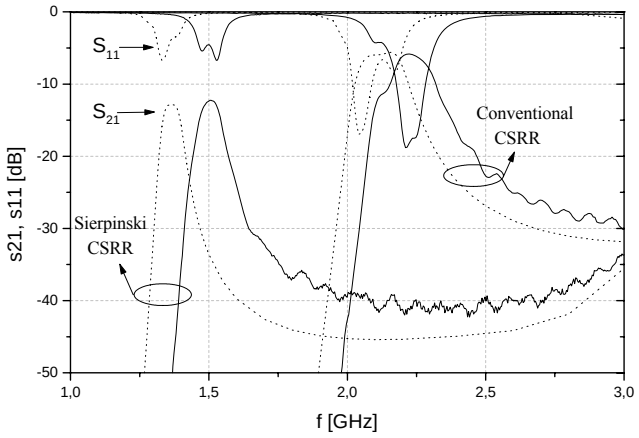

Fig. 13. Simulation (dotted line) and measurement (full line) results for lines that use square Sierpinski complementary split-ring resonators and complementary split-ring resonators.

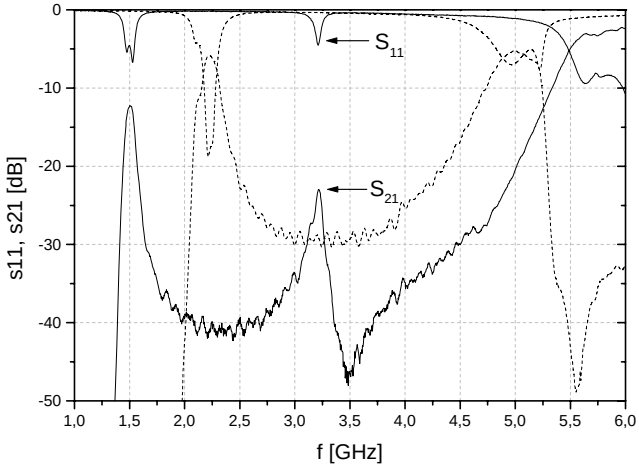

Fig. 14. Measurement results for the lines that use square Sierpinski complementary split-ring resonators (full line) and complementary split-ring resonators (dotted line) in wider frequency range.

B. Left-Handed Microstrip Lines That Use Unit Cells With Multiple Square Sierpinski Complementary Split-Ring Resonators

In order to validate simulation results, left-handed microstrip lines that use multiple square Sierpinski complementary split-ring resonators were fabricated. Photographs of top and bottom layers of the fabricated structures with N=3 and N=4 concentric square Sierpinski complementary split-ring resonators are shown in Fig. 15.

The measurement and simulation results of the proposed left-handed microstrip lines are compared in Fig. 16. A good agreement can be observed, except for a shift in frequency approximately equal to 10% that occurs in all cases. As in the previous case, this can be explained by the discrepancy between actual and simulated values of the dielectric constant and substrate thickness.

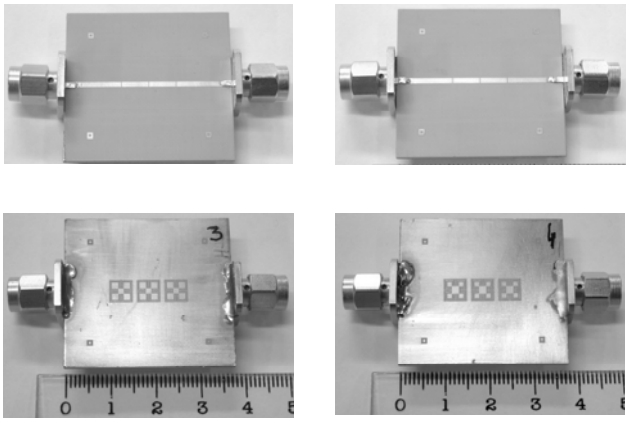

(a) (b)

Fig. 15. Top (upper) and bottom (lower) sides of the fabricated left-handed transmission lines that use unit cells with square Sierpinski complementary split-ring resonators: (a) N=3, (b) N=4.

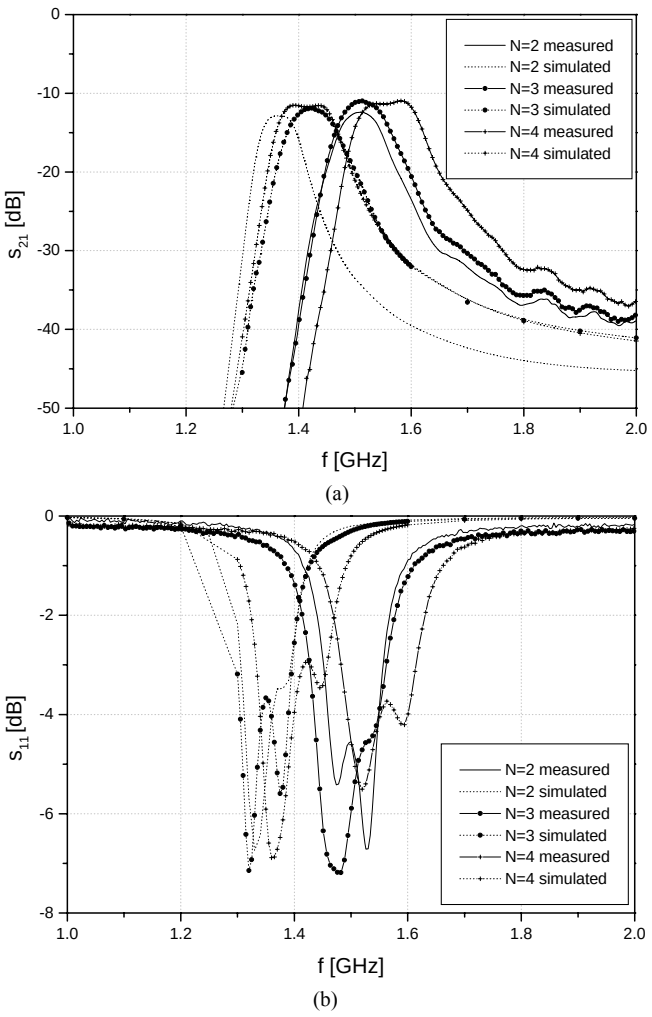

(a)

(b)

Fig. 16. Simulation (dotted lines) and measurement (full lines) results for left-handed microstrip lines that use N=2,3,4 square Sierpinski complementary split-ring resonators: (a) insertion loss, (b) return loss.

Fig. 17 shows the measurement results up to 6 GHz, for all proposed left-handed lines. It can be seen that all configurations show sharp transition on both sides of the first pass-band. As N increases, second harmonics are shifted towards higher frequencies. Furthermore, all structures successfully suppress a frequency band in the vicinity of the second harmonic of the quasi-static resonance of the rings, positioned at approximately $2f_{c1}$. In that way, wide and deep stop bands in the transmission characteristics are created.

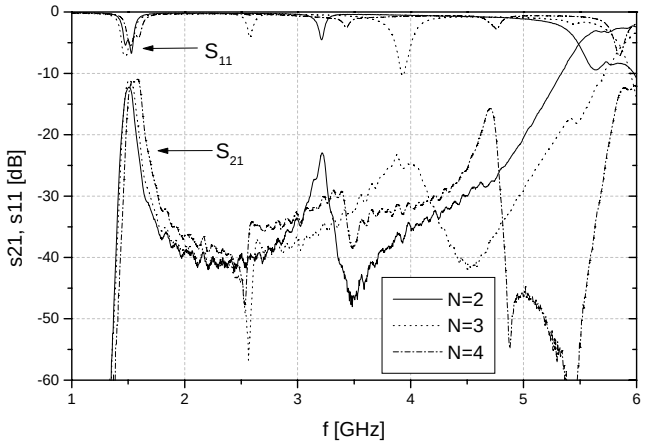

Fig. 17. Measurement results for the proposed left-handed microstrip lines that use *N=2,3,4* square Sierpinski complementary split-ring resonators in wider frequency range.

V. Conclusion

In this paper, novel complementary split-ring resonator geometries are presented, that use square Sierpinski fractal curves of the second and the third order. The topologies with different number of concentric rings are also analyzed, as well as the influence that several geometrical parameters have on the performances. It is shown that fractal geometries with the original dimensions perform better in terms of miniaturization then the modified ones, and better then similar but non-fractal structures.

Simulations and measurements show that the application of fractal geometries significantly lowers resonant frequency of the structure, therefore revealing high potential that fractal topologies have for the unit cell miniaturization. Due to the unique shape of the fractal curve, inductance of the double split-ring is increased for approximately 57% and its capacitance for more than 55%, for the same overall dimensions of the ring, in comparison to the conventional case. Furthermore, the improved frequency selectivity in the upper transition band is achieved.

Since fractal curves fill the space in an optimal manner, adding concentric split-rings changes the resonant frequency only for a few percents. However, the second harmonic is significantly shifted towards the higher frequencies when the number of concentric rings is increased, thus resulting in much wider stop bands. The proposed structures with multiple rings successfully suppress frequency bands positioned at approximately $2f_{c1}$. In this case, behaviour specific to fractal geometries is observed and explained: by adding concentric rings, the capacitance of the structure becomes dominant, instead of the inductance. Dispersion diagrams further illustrate different behaviour of the lines that use multiple conventional and fractal complementary split-rings.

The efficiency of excitation of square Sierpinski complementary split-ring resonator by axial electric field is also analysed. Although the centre of the proposed unit cell is partially occupied by the ring, this does not significantly influence the excitation. The increased insertion loss that fractal rings exhibit in comparison to the conventional ones is not due to deteriorated excitation, but is the consequence of the significantly increased length of the fractal ring.

When the order of the fractal curve used for complementary split-ring resonator design is increased, while the overall dimensions are fixed, the resonant frequency can be lowered for 44% in respect to the conventional case. In this way, even more compact unit cells with the dimensions $\lambda_g/20$ x $\lambda_g/20$ can be designed.

References

[1] V. G. Veselago, "The electrodynamics of substances with simultaneously negative values of ε and μ," *Soviet Physics Uspekhi*, vol. 10, pp.509–514, 1968.

[2] J. B. Pendry, A. J. Hoden, W. J. Stewart, and I. Youngs, "Extremly low frequency plasmons in metallic mesostructures," *Physical Review Letters*, vol. 76, num. 25, pp. 4773-4776, 17 June 1996.

[3] J. B. Pendry, A. J. Holden, D. J. Robbins, and W. J. Stewart, "Magnetism from conductors and enchanced nonlinear phenomena," *IEEE Trans. on Microwave Theory and Techniques*, vol. 47, no. 11, pp. 2075-2084, November 1999.

[4] R. A. Shelby, D. R. Smith, S. Schultz, "Experimental verification of a negative index of refraction," *Science*, vol. 292, pp. 77-79, 2001.

[5] R. Marqués, J. Martel, F. Mesa, and F. Medina, "Left handed media simulation and transmission of EM waves in sub-wavelength SRR-loaded metallic waveguides", *Phys. Rev. Lett*., vol 89, pp. 183901-03, 2002.

[6] F. Martín, F. Falcone, J. Bonache, R. Marqués, and M. Sorolla, "Miniaturized coplanar waveguide stop band filters based on multiple tuned split ring resonators", *IEEE Microwave Wireless Comp. Lett.*, vol. 13, pp. 511-513, December 2003.

[7] J. Baena, J. Bonache, F. Martin, R. Marqués, F. Falcone, T. Loptigei, M. Laso, J. Garcia, I. Gil, M. Portillo, and M. Sorrola, "Equivalent-circuit models for split-ring resonators and complementary split-ring resonatos coupled to planar transmission lines," *IEEE Trans. on Microwave Theory and Techniques*, vol. 53, no. 4, pp. 1451-1461, April 2005.

[8] R. Marqués, F. Medina, and R. Idrissi, "Role of bianisotropy in negative permeability and left handed metamaterials," *Phys. Rev. B, Condens. Matter*, vol. 65, pp. 144 441–144 446, April 2002.

[9] J. Baena, R. Marqués, F. Medina, and J. Martel, "Artificial magnetic metamaterial design by using spiral resonators," *Phys. Rev. B, Condens. Matter*, vol. 69, pp. 14 402–14 402, January 2004.

[10] F. Falcone, F. Martín, J. Bonache, M. Laso, J. García-García, J. Baena, R. Marqués, and M. Sorolla, "Stopband and band pass characteristics in coplanar waveguides coupled to spiral resonators," *Microwave Opt. Technol. Lett.*, vol. 42, pp. 386–388, September 2004.

[11] V. Crnojević-Bengin, V. Radonić, and B. Jokanović, "Left-handed microstrip lines with multiple complementary split-ring and spiral resonators," *Microwave Opt. Technol. Lett.*, vol. 49, no.6, pp.1391-1395, June 2007.

[12] F. Bilotti, A. Toscano, L. Vegni, "Design of spiral and multiple split-ring resonators for the realization of miniaturized metamaterial samples," *IEEE Trans. Antennas Propag.*, vol. 55, no. 8, pp. 2258-2267, August 2007.

[13] F. Falcone, T. Lopetegi, M. A. G. Laso, J. D. Baena, J. Bonache, M. Beruete, R. Marqués, F. Martín, and M. Sorolla, "Babinet principle applied to metasurface and metamaterial design," Phys. Rev. Lett., vol. 93, pp. 197 401(1)–197 401(4), November 2004.

[14] V. Crnojević-Bengin, V. Radonić, and B. Jokanović, "Complementary Split Ring Resonators Using Square Sierpinski Fractal Curves," *Proc. Of*

European Microwave Conference EuMC 2006, paper #1052, EuMCPoster1-59, September 2006.
[15] G. Peano, "Sur une courbe qui remplit toute une aire plaine," *Math. Ann.*, 36, 1890.
[16] V. Crnojević-Bengin, "Novel compact microstrip resonators with multiple 2-D Hilbert fractal curves," *Microwave and Optical Technology Letters*, vol. 48, no.2, pp.270-273, February 2006.
[17] V. Crnojević-Bengin, and Đ. Budimir, "Novel 3-D Hilbert microstip resonators," *Microwave and Optical Technology Letters*, vol. 46, no. 3, pp 195-197, August 2005.
[18] K.J. Vinoy, K.A. Jose, V.K. Varadan, and V.V. Varadan, "Hilbert curve fractal antenna: A small resonant antenna for VHF/UHF applications," *Microwave Opt. Technol Lett*., vol. 29 , pp. 215–219. 2001.
[19] J. Anguera, C. Puente, E. Martı´nez, and E. Rozan, "The fractal Hilbert monopole: A two-dimensional wire," *Microwave Opt. Technol Lett.,* vol. 36, pp. 102–104. 2003.
[20] J. Zhu, A. Hoorfar, and N. Engheta, "Bandwidth, cross-polarization, and feed-point characteristics of matched Hilbert antennas," *IEEE Antennas Wireless Propag Lett.*, vol. 2, pp. 2–5, 2003.
[21] J. Zhu, A. Hoorfar, and N. Engheta, "Peano antennas," *IEEE Antennas Wireless Propag Lett.*, vol. 3, pp. 71-74, 2004.
[22] E.A. Parker, and A.N.A. El Sheikh, "Convoluted array elements and reduced size unit cells for frequency-selective surfaces," *IEE Proc. Microwave Antennas Propag*, vol. 138, pp. 19–22, 1991.
[23] J. McVay, N. Engheta, and A. Hoorfar, "High-impedance metamaterial surfaces using Hilbert-curve inclusions," *IEEE Microwave and Wireless Components Letters*, vol. 14, no. 3, pp 130-132, March 2004.
[24] J. McVay, A. Hoorfar, and N. Engheta, "Peano high-impedance surfaces," *Radio Sci*, 40, RS6S03, 2005.
[25] J. McVay, N. Engheta, and A. Hoorfar, "Numerical study and parameter estimation for double-negative metamaterials with Hilbert-curve inclusions," *Proceedings of 2005 IEEE Antennas Propagation Society International Symposium*, Washington, DC, vol. 2B, pp. 328–331, July 2005.
[26] J. McVay, A. Hoorfar, and N. Engheta, "Space-filling curve RFID tags," *Proceedings of IEEE Radio and Wireless Symposium*, San Diego, CA, pp. 199–202, January 2006.
[27] V. Pierro, J. McVay, V. Galdi, A. Hoorfar, N. Engheta, and I. M. Pinto, "Metamaterial inclusions based on grid-graph Hamiltonian paths," *Microwave Opt. Technol. Lett.*, vol. 48, no. 12, pp. 2520–2524, December 2006.

Vesna Crnojevic-Bengin (SM'96, M'06) received Dipl. Ing. degree in Telecommunications and Electronics from the Faculty of Technical Sciences, University of Novi Sad, Serbia in 1994, and MSc degree from the Faculty of Electrical Engineering, University of Belgrade, Serbia in 1997. She received PhD degree in electronics and microwave engineering from the University of Novi Sad in 2006, where she is currently an Assistant Professor.

Dr Crnojevic-Bengin is the recipient of the YU MTT Award for Scientific Contribution in 2005. Her main research interests include application of fractal curves in the design of microwave passive devices and metamaterials.

Vasa Radonic (S'06) was born in Novi Sad, Serbia in 1979. He received the B.Sc. and M.Sc. degrees from the Faculty of Technical Sciences, University of Novi Sad, Serbia, in 2004 and 2007 respectively, where he is currently working towards the Ph.D. degree in the field of metamaterials.

Mr. Radonic is employed as Research Assistant at the Faculty of Technical Sciences, University of Novi Sad, Serbia.

Branka Jokanovic (M'89) received Dipl. Ing. degree from the Faculty of Electrical Engineering, University of Belgrade in 1977, and MSc and PhD degrees at the same University in 1988 and 1999, respectively. She was one of the founders of the Yugoslav IEEE MTT-S Chapter and its chairperson in the period 1989-2000. She also initiated foundation of the Yugoslav Association for Microwave Techniques and Technology in 1992, and publishing of Microwave Review, Serbian journal of the national importance in 1994, where she served as the editor for six years. B. Jokanovic is currently Head of Research Department of IMTEL Communications responsible for the development of a new generation of microwave links based on nanotechnology. She is the president of Scientific Council of IMTEL Communications and member of the Advisory Board of RATEL (Republic Agency for Telecommunications).

Dr Jokanovic is the recipient of the IMTEL Institute Award for Scientific Contribution in 1996, the IEEE Third Millennium Award in 2000 and YU MTT Distinguished Service Award in 2005. She has authored or co-authored about 100 conference, letter and journal papers, and one book. Her current research interests include novel metamaterials for millimeter-wave and ultra-wideband (UWB) applications and nanostructured materials for broadband wireless systems.